MOLECULAR AND CELLULAR BIOLOGY, May 2007, p. 3625–3639 Vol. 27, No. 10
0270-7306/07/$08.00+0 doi:10.1128/MCB.02295-06
Copyright © 2007, American Society for Microbiology. All Rights Reserved.

Novel Role for Mitochondria: Protein Kinase Cθ-Dependent Oxidative Signaling Organelles in Activation-Induced T-Cell Death[▽]

Marcin Kamiński, Michael Kießling, Dorothee Süss, Peter H. Krammer, and Karsten Gülow*

Tumor Immunology Program, German Cancer Research Center (DKFZ), Heidelberg, Germany

Received 8 December 2006/Returned for modification 31 January 2007/Accepted 26 February 2007

Reactive oxygen species (ROS) play a key role in regulation of activation-induced T-cell death (AICD) by induction of CD95L expression. However, the molecular source and the signaling steps necessary for ROS production are largely unknown. Here, we show that the proximal T-cell receptor-signaling machinery, including ZAP70 (zeta chain-associated protein kinase 70), LAT (linker of activated T cells), SLP76 (SH2 domain-containing leukocyte protein of 76 kDa), PLCγ1 (phospholipase Cγ1), and PKCθ (protein kinase Cθ), are crucial for ROS production. PKCθ is translocated to the mitochondria. By using cells depleted of mitochondrial DNA, we identified the mitochondria as the source of activation-induced ROS. Inhibition of mitochondrial electron transport complex I assembly by small interfering RNA (siRNA)-mediated knockdown of the chaperone NDUFAF1 resulted in a block of ROS production. Complex I-derived ROS are converted into a hydrogen peroxide signal by the mitochondrial superoxide dismutase. This signal is essential for CD95L expression, as inhibition of complex I assembly by NDUFAF1-specific siRNA prevents AICD. Similar results were obtained when metformin, an antidiabetic drug and mild complex I inhibitor, was used. Thus, we demonstrate for the first time that PKCθ-dependent ROS generation by mitochondrial complex I is essential for AICD.

Because CD95L expression is crucial for the induction of activation-induced T-cell death (AICD), efforts have been made to explore the connection between T-cell receptor (TCR) signaling and regulation of CD95L transcription. Following TCR engagement, ZAP70 (zeta chain-associated protein kinase 70) is activated (11). ZAP70 phosphorylates the adaptor protein LAT (linker of activated T cells) (19), which recruits PLCγ1 (phospholipase Cγ1) subsequently. The activation of PLCγ1 results in the generation of inositol 3,4,5-triphosphate (IP_3) and diacylglycerol (DAG). IP_3 mediates an increase in cytosolic calcium (Ca^{2+}), whereas DAG activates protein kinase C (PKC). The rise in cytosolic Ca^{2+} causes activation of the transcription factor NF-AT (nuclear factor of activated T cells) (69), one of the key regulators of CD95L expression (41). In addition, reactive oxygen species (ROS) are shown to be crucial for activation-induced CD95L expression (7, 15, 25), possibly via the ROS-inducible transcription factors NF-κB and AP-1 (17). Recently, we demonstrated that a hydrogen peroxide (H_2O_2)-mediated signal combined with simultaneous Ca^{2+} influx into the cytosol constitutes the minimal requirement for CD95L expression (25). However, the molecular source of TCR-induced ROS remains largely unclear. Aerobic organisms produce ROS by several means: in mitochondria as a by-product of respiration (63), at the endoplasmic reticulum by cytochrome P450 (50), in the cytoplasm by xanthine oxidase (20), at the plasma membrane by NADPH oxidases (35, 46) and phospholipases (54), and in peroxisomes (56). Recently, the phagocytic NADPH oxidase (NOX2) was shown to be one source for TCR-triggered ROS. However, NOX2 is not the only source for activation-induced ROS (30). Following T-cell activation, respiratory activity increases (21) and mitochondrial ROS production may be enhanced (27). In addition, there are hints supporting a possible role of the mitochondrial electron transport chain (ETC) and cytochrome P450 as origins of activation-induced ROS (7). Thus, mitochondrial involvement in activation-induced ROS generation could be addressed.

In the present study, we investigated and identified the molecular signaling pathway of TCR-induced ROS generation. Here, we demonstrate for the first time that the proximal TCR signaling machinery is essential for ROS production. Cells deficient in ZAP70, LAT, SLP76 (SH2 domain-containing leukocyte protein of 76 kDa), or PLCγ1 revealed no oxidative signal upon TCR stimulation. The TCR signaling machinery could be bypassed via the DAG mimetic phorbol 12-myristate 13-acetate (PMA), pointing to a role of Ca^{2+}-independent PKCs inducing oxidative signals. Downmodulation of PKC levels by small interfering RNA (siRNA) oligonucleotides revealed that activation-induced ROS generation and CD95L expression are PKCθ dependent. Moreover, we demonstrate that PKCθ is translocated to the mitochondria and/or associated membranes upon PMA treatment. By using mitochondrial DNA (mtDNA)-depleted cells (pseudo-[rho^0] cells) we show that mitochondrial function is crucial for ROS generation and subsequent AICD. Moreover, by employing specific inhibitors and siRNA-mediated knockdown of NDUFAF1, a chaperone essential for mitochondrial ETC complex I assembly (66), we demonstrate that complex I is the molecular source of activation-induced ROS in T cells. In addition, we show that the ROS produced by complex I are needed for activation of NOX2. Thus, the mitochondria are the superior source of activation-induced ROS. Finally, we prove the physiological

* Corresponding author. Mailing address: Tumor Immunology Program, German Cancer Research Center (DKFZ), Im Neuenheimer Feld 280, 69120 Heidelberg, Germany. Phone: 49 6221 423765. Fax: 49 6221 411715. E-mail: k.guelow@dkfz.de.

▽ Published ahead of print on 5 March 2007.

role of complex I-induced ROS by inhibition of AICD via downmodulation of NDUFAF1 expression and application of metformin, a common antidiabetic drug and mild inhibitor of complex I (6, 18). In conclusion, the data presented here provide new insights into the molecular mechanism of AICD, suggesting a possible therapeutic role of ROS scavengers and complex I inhibitors in the treatment of CD95/CD95L-dependent disorders.

MATERIALS AND METHODS

Chemicals. Dichlorodihydrofluorescein diacetate (DCFDA) was obtained from Molecular Probes, Germany. Cell-permeable, myristoylated pseudosubstrate peptide inhibitors (general anti-PKC and anti-PKCθ) were purchased from Calbiochem, Germany. Primary antibodies against human PKCδ and PKCθ were supplied by BD Transduction Laboratories, Germany. Primary antibodies against human mitochondrial superoxide dismutase (MnSOD) and LAT were obtained from Upstate Biotechnology. The primary antibody against human ZnCuSOD was purchased from Santa Cruz Biotechnology, Germany. The neutralizing anti-CD95L antibody Nok1 was obtained from BD Pharmingen, Germany. All other chemicals and primary antibodies against human tubulin α were supplied by Sigma-Aldrich, Germany. The agonistic monoclonal antibody anti-Apo-1 (mouse immunoglobulin G3), recognizing an extracellular epitope of CD95 (Apo1/Fas) (62), and the monoclonal anti-CD3 antibody OKT3 (25) were prepared as described previously.

Cell culture. Jurkat J16-145 is a subclone of the human T-lymphoblastoid cell line Jurkat J16 (25). J.CaM2 is a LAT-negative Jurkat cell line, and J.CaM2/LAT is the control cell line retransfected with LAT (19). P116 is a ZAP70-negative Jurkat cell line (68), and P116cl.39 is the retransfected control cell line. J14 is a SLP76-deficient cell line, and J14 76-11is the retransfected control cell line (37). J.γ1 is a PLCγ1-deficient Jurkat cell line, and J.γ1/PLCγ1 is the retransfected control cell line (29). Jurkat cells were cultured in Iscove modified Dulbecco medium (IMDM) supplemented with 10% fetal calf serum (FCS).

Generation of pseudo-[*rho*^{0}] cells. Cells depleted of mtDNA were generated as described previously (12, 36) with minor modifications. Briefly, Jurkat J16-145 cells were cultured in IMDM supplemented with ethidium bromide (250 ng/ml) for up to 21 days. Ethidium bromide accumulates in much higher concentrations in the mitochondrial matrix than in the nucleus. Therefore, it can be used to selectively inhibit mtDNA replication. The amount of mtDNA was examined by isolation of DNA followed by PCR specific for the mitochondrial origin of replication. The amplified product spanned the mitochondrial origin of replication of the mtDNA heavy strand between positions 15868 and 754, as follows: sense, 5′-GAAAACAAAATACTCAAATGGGCC-3′; antisense, 5′-CCTTTTG ATCGTGGTGATTTAGAGGG-3′. Cells depleted of mtDNA rely energetically mainly on glycolysis and have impaired nucleotide metabolism. Therefore, pseudo-[*rho*^{0}] cells were further cultured in IMDM supplemented with ethidium bromide (250 ng/ml), uridine (50 μg/ml), and sodium pyruvate (110 mg/ml). Because the cells were not completely deficient in mtDNA, they are referred to as pseudo-[*rho*^{0}] cells (12). To reconstitute mtDNA content, pseudo-[*rho*^{0}] cells were transferred to standard medium. Cells recovered to normal phenotype in 21 to 23 days.

Isolation of total cellular DNA. Jurkat J16-145 cells were lysed for 1 h at 55°C in 0.2 M sodium acetate–6.25% sodium dodecyl sulfate (SDS) solution containing 250 μg/ml proteinase K. Genomic DNA was isolated by phenol-chloroform extraction.

Isolation of human peripheral T cells. Human peripheral T cells were prepared by Ficoll-Paque density centrifugation, followed by rosetting with 2-aminoethylisothyouronium-bromide-treated sheep red blood cells, as described previously (25). For activation, resting T cells were cultured at a concentration of 2×10^6 cells/ml with 1 μg/ml phytohemagglutinin for 16 h. Next, T cells were cultured in RPMI 1640 supplemented with 10% FCS and 25 U/ml interleukin 2 for 6 days (day 6 T cells), as described previously (25). All experiments were performed with T cells isolated from at least three different, healthy donors.

Isolation of human polymorphonuclear cells. Neutrophils from healthy individuals were prepared by Polymorphprep density centrifugation according to the manufacturer's instructions (Axis-Shield, Norway). All experiments were performed with neutrophils isolated from at least three different, healthy donors.

Assessment of cell death. To induce CD95L expression and/or subsequent apoptosis, cells were stimulated with anti-CD3 antibody (OKT3, 30 μg/ml) or PMA (10 ng/ml) and ionomycin (1 μM). Cell death was assessed by a drop in the forward-to-side-scatter (FSC/SSC) profile in comparison to living cells and recalculated to "specific cell death" as described previously (25).

Determination of anti-CD3- and PMA-induced ROS generation. Jurkat cells were stimulated either with plate-bound anti-CD3 (OKT3, 30 μg/ml) or with PMA (10 ng/ml) for 30 min and stained with the oxidation-sensitive dye H_2DCFDA (5 μM). Since activation-induced ROS generation in human T cells was maximal at 30 min of stimulation (25), this time point was chosen for all experiments. Incubation was terminated by a wash with ice-cold phosphate-buffered saline. ROS generation was determined by fluorescence-activate cell sorting (FACS) and quantified as the increase in mean fluorescence intensity (MFI), calculated by the following formula: increase in MFI (%) = $[(MFI_{stimulated} - MFI_{unstimulated})/MFI_{unstimulated}] \times 100$ (as described in reference 15). Cells were preincubated with inhibitors for 5 min prior to stimulation, with the exception of anti-PKC peptide inhibitors (20 min) and metformin (1 h). All experiments were performed in triplicate. The results shown are representative of at least three independent experiments.

ATP determination. Cells were lysed by freezing and thawing. Cellular ATP was measured according to the manufacturer's instructions (Molecular Probes, Germany).

Mitochondrial isolation and Western blot analysis. Crude mitochondrial fractions (containing membrane impurities) and cytoplasmic fractions were isolated with the Mitochondria Isolation Kit (Pierce), according to the manufacturer's instructions. Next, membranes were separated from mitochondria by isopycnic 0.8 to 2 M sucrose gradient centrifugation for 2 h at $80{,}000 \times g$. Figure 4A contains a schematic diagram of the purification procedure. Cells were lysed in radioimmunoprecipitation assay lysis buffer (60 mM NaCl, 25 mM Tris-HCl, 0.5% deoxycholate, 1 mM dithiothreitol, and Halt protease inhibitor cocktail [Pierce]), and the protein concentration was measured by the bicinchoninic acid assay (Pierce). SDS-polyacrylamide gel electrophoresis (PAGE) and Western blot analysis were performed as described previously (24). Band intensities were quantified by standard scanning densitometry with the NIH Image program, version 1.36b.

RNA preparation and semiquantitative RT-PCR. RNA was isolated with TRIzol reagent (Invitrogen, Germany) according to the manufacturer's instructions. Total RNA (5 μg) was reverse transcribed with a reverse transcription (RT)-PCR kit (Applied Biosystems, Germany). Aliquots were amplified by PCR as described previously (25). Primers for detection of CD95L, β-actin, and NDUFAF1 were used as described previously (25, 40, 66). Primers used for amplification of MnSOD (*SOD2*) and Zn/CuSOD (*SOD1*) transcripts were as follows: MnSOD sense, 5′-CTTCAGCCTGCACTGAAGTTCAAT-3′; antisense, 5′-CTGAAGGTAGTAAGCGTGCTCCC-3′; Zn/CuSOD sense, 5′-GCG ACGAAGGCCGTGTGCGTGC-3′; antisense, 5′-CTAGAATTTGCGGTGGA CGATGGAGGG-3′.

Quantitative PCR. The primers and fluorescently labeled probes used for quantitative PCR were as follows: CD95L sense, 5′-AAAGTGGCCCATTTAA CAGGC-3′; antisense, 5′-AAAGCAGGACAATTCCATAGGTG-3′; probe, 5′-TCCAACTCAAGGTCCATGCCTCTGG-3′; β-actin sense, 5′-ACCCACACT GTGCCCATCTACGA-3′; antisense, 5′-CAGCGGAACCGCTCATTGCCAA TGG-3′; probe, 5′-ATGCCCTCCCCCATGCCATCCTGCGT-3′. The PCR mixture (PCR kit from Eurogentech, Belgium) contained 80 μg of reverse transcribed cDNA, 1.25 ± 7.5 pM forward primers, 22.5 pM reverse primers, and 5 pM probe. For each sample, three PCRs were performed. The resulting relative increase in reporter fluorescent dye emission was monitored by the TaqMan system (GeneAmp 5700 sequence detection system and software; Perkin Elmer, Foster City, CA). The levels of the CD95L and CD95 mRNAs relative to β-actin mRNA were calculated by the following formula: relative mRNA expression = $2^{-(C_T \text{ of CD95L} - C_T \text{ of β-actin})}$, where C_T is the threshold cycle value.

Transfection and siRNA-mediated knockdown. Jurkat T cells and primary human T cells were transfected by lipofection (HiPerfect; QIAGEN, Germany) with negative control siRNA oligonucleotides (unlabeled or Alexa 488-labeled nonsilencing siRNA; QIAGEN, Germany) and siRNA oligonucleotides specific for human NDUFAF1 (oligo#1 antisense strand, 5′-ACUAACAUCAGGCUU CUCCdTdT-3′; oligo#2 antisense strand, 5′-UAACUAUACAUCUGAUUCG dTdT-3′) or siRNA oligonucleotides specific for human PKCδ (Hs_PKKCD_11_ HP) and PKCθ (Hs_PRKCQ_5_HP) (QIAGEN, Germany). Transfection was performed with 2×10^5 cells, 9 μl of transfection reagent, and different amounts of siRNA oligonucleotides ranging from 75 nM to 900 nM, according to the manufacturer's instructions. Transfected cells were rested for 48 h before being subjected to further experiments.

Measurement of MnSOD activity. MnSOD activity was determined with a commercial kit (Dojindo Molecular Technologies, Japan). Cells (1.5×10^7) were stimulated with plate-bound anti-CD3 antibody (OKT3, 30 μg/ml) or with PMA (10 ng/ml) for different time periods. Cells were harvested and lysed by freezing and thawing. The protein content was adjusted to 1 mg/ml, and SOD activity was measured with a photometer according to the manufacturer's instructions. MnSOD

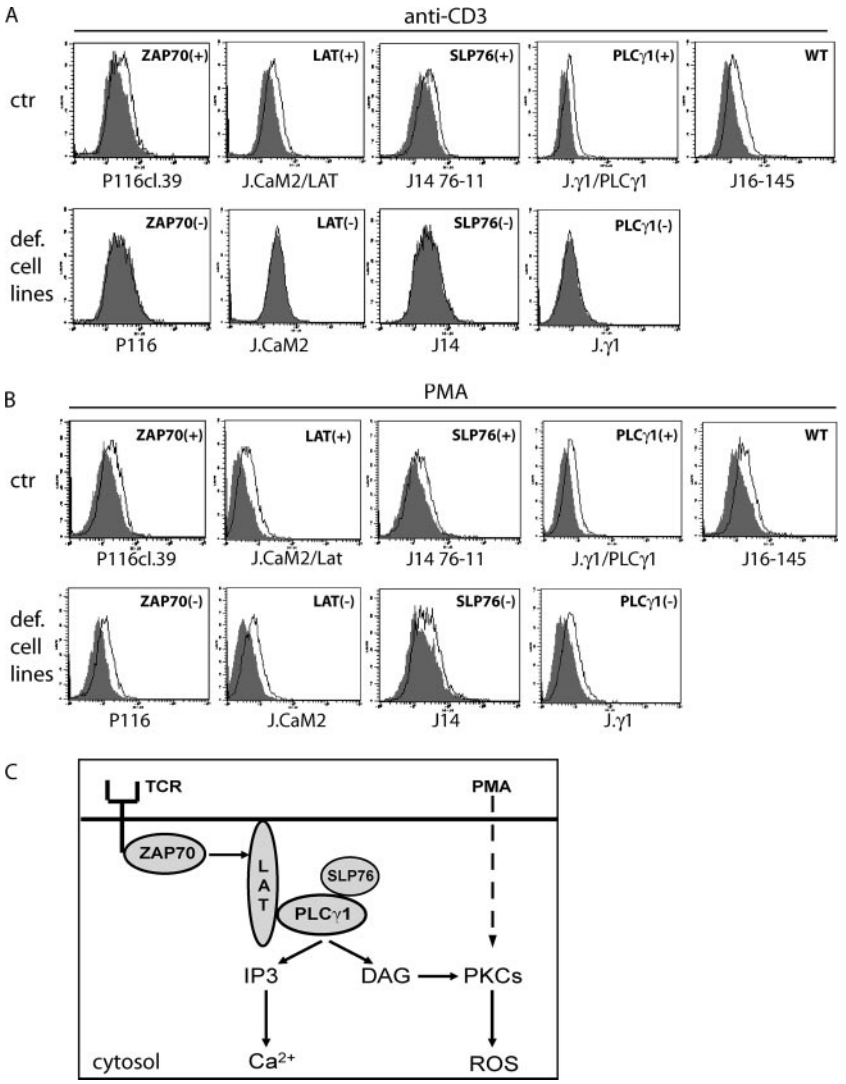

FIG. 1. Activation-induced ROS generation depends on the proximal TCR signaling machinery. (A and B) Jurkat J16-145, P116 (ZAP70-negative Jurkat), P116cl.39 (ZAP70-retransfected control), J.CaM2 (LAT-negative Jurkat), J.CaM2/LAT (LAT-retransfected control), J14 (SLP76-deficient Jurkat), J14 76-11 (SLP76-retransfected control), J.γ1 (PLCγ1-deficient Jurkat), and J.γ1/PLCγ1 (PLCγ1-retransfected control) cells were stimulated via plate-bound anti-CD3 antibodies (A) or with PMA (B) for 30 min. Thereafter, cells were stained with DCFDA. Representative FACS profiles for activation-induced DCFDA oxidation are shown. ctr, retransfected control, def. cell lines, lines deficient in signaling molecules. (C) Schematic diagram of TCR signaling.

activity was assessed after blocking of the background activity of ZnCuSOD by the addition of 1 mM KCN to the reaction mixture.

RESULTS

TCR-induced ROS generation depends on the proximal TCR signaling machinery. Previous studies indicate that TCR stimulation leads to generation of an oxidative signal involving H_2O_2 (15, 25). This H_2O_2 signal is vital for the initiation of CD95L promoter activity, CD95L expression, and AICD (25). In order to identify the components of the transduction cascade mediating ROS generation, we used cells deficient in TCR-signaling molecules. Jurkat cell lines deficient in ZAP70 (68), LAT (19), SLP76 (37), and PLCγ1 (29) were stained with DCFDA and stimulated with plate-bound anti-CD3 antibodies for 30 min. All deficient cell lines did not display any oxidative signal, whereas retransfected controls showed a clear increase of ROS upon TCR stimulation (Fig. 1A). Thus, we conclude that TCR-induced generation of ROS depends on ZAP70, LAT, SLP76, and PLCγ1 (Fig. 1C). As PLCγ1 activation results in triggering of PKCs, we investigated a possible role of PKCs in oxidative signaling by treating the deficient cell lines with PMA, a PKC activator, which bypasses ZAP70, LAT, SLP76, and PLCγ1. Remarkably, all deficient cell lines revealed a PMA-induced oxidative signal (Fig. 1B). PMA induces an oxidative signal without influencing the intracellular Ca^{2+} level (25). This implicates an involvement of Ca^{2+}-independent PKCs in TCR-induced oxidative signaling (Fig. 1C).

PKCθ is required for activation-induced generation of ROS. To further corroborate an involvement of PKCs in activation-induced ROS formation, cells stimulated via PMA and plate-

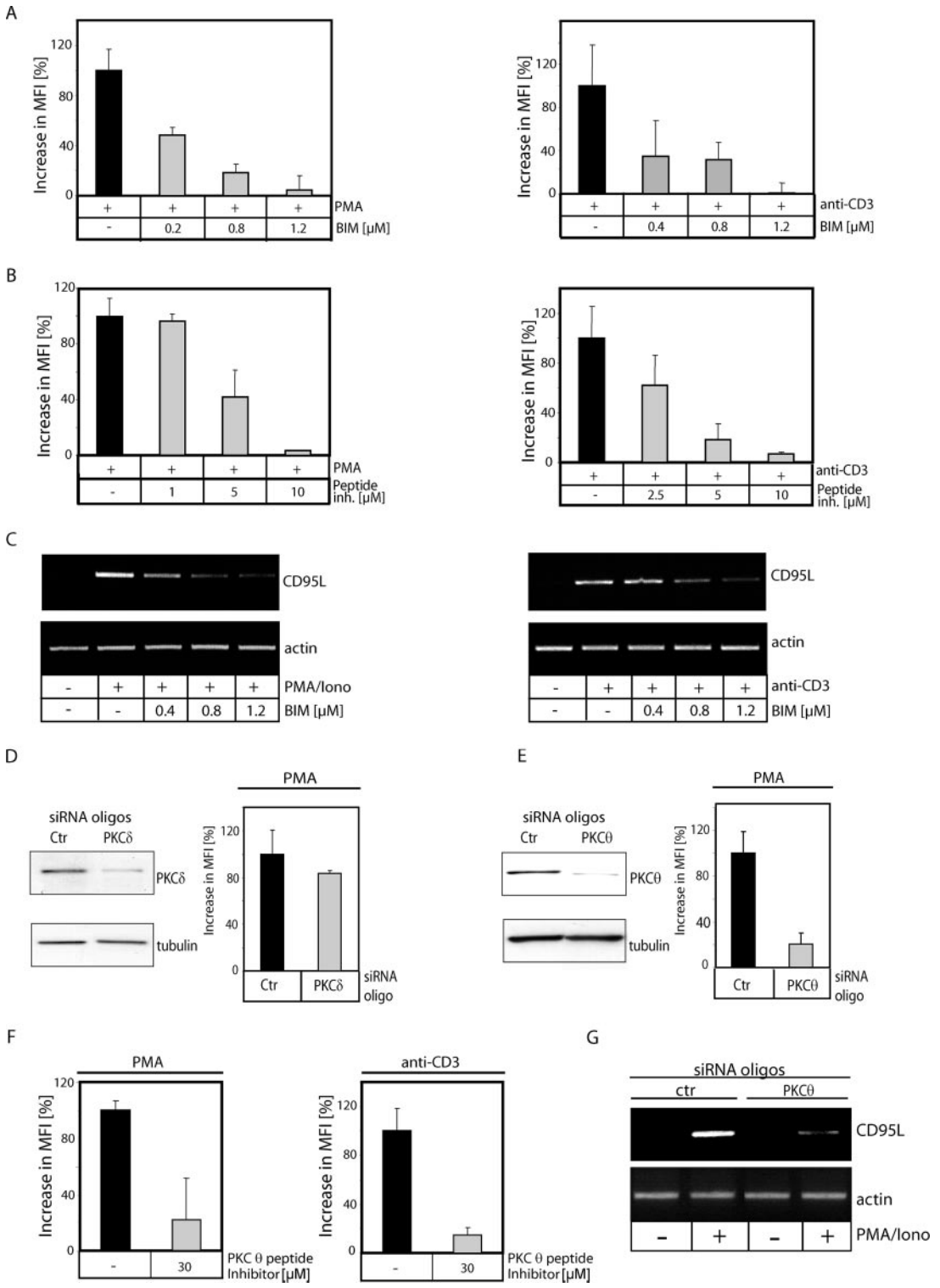

FIG. 2. PKCθ is required for activation-induced generation of ROS. (A) J16-145 cells were pretreated with the indicated amounts of the PKC inhibitor BIM and stimulated with PMA (left) or plate-bound anti-CD3 antibodies (right) for 30 min. Cells were stained with DCFDA and analyzed by FACS. Data shown as the percent increase in MFI. (B) J16-145 cells were pretreated with the indicated amounts of a general PKC pseudosubstrate peptide inhibitor, stained with DCFDA, and stimulated with PMA (left) or plate-bound anti-CD3 antibodies (right) for 30 min. ROS levels were measured as for panel A. (C) J16-145 Jurkat cells were pretreated with the indicated amounts of the PKC inhibitor BIM and stimulated with PMA/ionomycin (left) or plate-bound anti-CD3 antibodies (right). After 1 h, RNA was isolated, reverse transcribed, and amplified with CD95L- and actin-specific primers. (D) Jurkat J16-145 cells were transfected with 900 nM concentrations of scrambled (Ctr) or PKCδ siRNA (PKCδ) oligonucleotides. After 96 h, transfected cells were lysed and analyzed by Western blotting for content of PKCδ (right) or stained with DCFDA, stimulated via PMA for 30 min, and subjected to FACS analysis (left); results are shown as the percent increase in MFI. (E) Jurkat

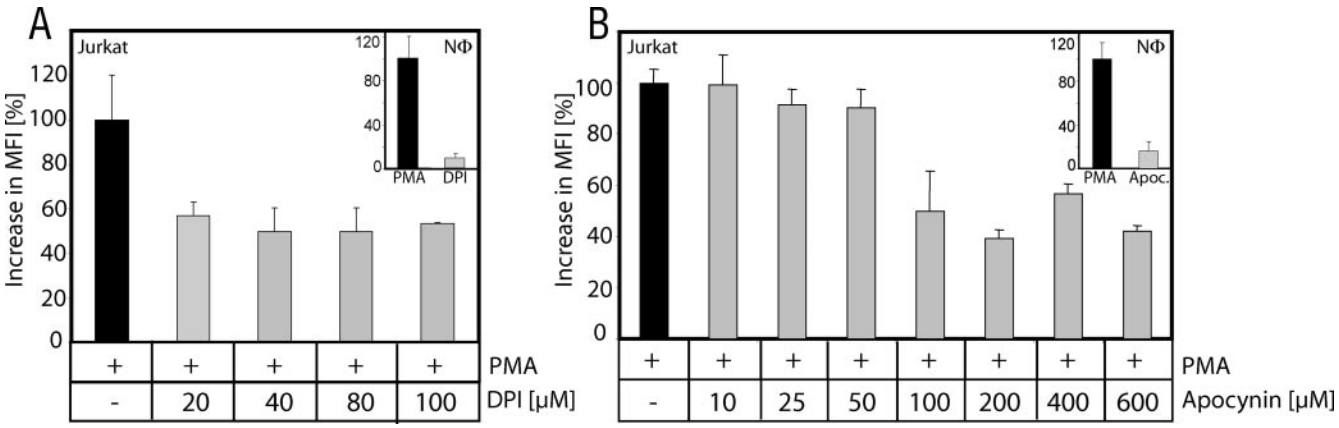

FIG. 3. Activation-induced ROS generation is partially NADPH oxidase dependent. Jurkat J16-145 cells were pretreated with the NADPH oxidase inhibitor DPI (A) or apocynin (B), stained with DCFDA, and stimulated with PMA for 30 min. Inserts show human neutrophils (NΦ) stimulated with PMA (10 ng/ml, 30 min) and cotreated with DPI (100 μM) (A) or apocynin (600 μM) (B) to inhibit the NADPH oxidase-dependent "oxidative burst." Data are presented as the FACS-measured increase in MFI of oxidized DCFDA.

bound anti-CD3 antibodies were pretreated with the general PKC inhibitor bisindolylmaleimide I (BIM) (Fig. 2A) or a PKC-specific peptide inhibitor (Fig. 2B). Both inhibitors blocked more than 95% of the oxidative signal. Since ROS cooperates with Ca^{2+} signaling for CD95L induction (25), we analyzed the impact of BIM on CD95L expression. Cells stimulated via anti-CD3 antibodies and PMA/ionomycin were pretreated with BIM. RNA was isolated, reverse transcribed, and amplified with CD95L-specific primers. In BIM-treated cells, a dose-dependent inhibition of CD95L expression was detectable (Fig. 2C). Considering that activation-induced oxidative signaling is inducible by PMA alone (Fig. 1B), we focused on Ca^{2+}-independent novel PKC isoforms (nPKC). It has been reported that PKCδ, an nPKC isoform, is involved in ROS generation in keratinocytes upon overexpression (39) and in PMA/ionomycin-treated myeloid leukemia cells (43). However, despite downmodulation of PKCδ via siRNA, the oxidative signal was not significantly affected (<20% decrease) (Fig. 2D). This implies that PKCδ plays only a minor role in the generation of activation-induced ROS. PKCθ is unique among the nPKC isoforms because it is indispensable for T-cell development and activation (48, 59, 64). To analyze the impact of PKCθ on activation-induced ROS production, cells were transfected with PKCθ siRNA oligonucleotides (Fig. 2E). More than 80% of the PMA-induced oxidative signal was inhibited in cells transfected with PKCθ siRNA oligonucleotides compared to the control. These data were further confirmed by treatment of Jurkat cells with a PKCθ-specific peptide inhibitor, which significantly reduced the TCR- and the PMA-induced ROS levels (Fig. 2F). Moreover, siRNA-mediated downmodulation of PKCθ results in an inhibition of CD95L expression (Fig. 2G). Thus, we conclude that PKCθ is crucial for activation-induced ROS formation and CD95L expression.

Activation-induced ROS generation is partially NADPH oxidase dependent. Recently, it has been shown in NOX2-deficient mice that TCR-induced ROS generation is, at least partially, dependent on NOX2 (30). Here, we analyzed a potential role of NADPH oxidases in human T cells. Jurkat cells were preincubated with DPI, a rather unspecific but commonly used NADPH oxidase inhibitor (14, 42, 55, 57, 60), or the specific NADPH oxidase inhibitor apocynin (61) and thereafter treated with PMA as an NADPH oxidase activator. Application of both DPI and apocynin showed only a moderate effect on PMA-induced ROS generation in Jurkat cells (Fig. 3). To control whether the applied amounts of inhibitor are sufficient to block NADPH oxidase, freshly isolated human neutrophils were treated with PMA (10 ng/ml) and cotreated with DPI and apocynin. PMA induces a massive NADPH oxidase-dependent ROS release in neutrophils called "oxidative burst." The "oxidative burst" could be inhibited almost completely (up to 91% inhibition) by application of 100 μM DPI or 600 μM apocynin. In Jurkat cells, the same amounts of inhibitor block not more than 60% of the PMA-induced oxidative signal (Fig. 3). Since downmodulation of PKCθ expression inhibited more than 80% of the oxidative signal (Fig. 2E), the existence of an additional PKCθ-dependent source of ROS in human T cells must be postulated.

Cells depleted of mtDNA show an impaired activation-induced ROS generation and AICD. Besides NOX2, mitochondria are a prominent source of ROS. It has been reported that upon PMA treatment, PKCδ can be translocated into/to mitochondria (39, 43). To determine whether PKCθ is translocated

J16-145 cells were transfected with 900 nM concentrations of scrambled (Ctr) or PKCθ siRNA (PKCθ) oligonucleotides. At 96 h after transfection, cells were analyzed as described for panel D. Shown are Western blots for PKCθ content (left) and PMA-induced DCFDA oxidation (right). (F) Jurkat J16-145 cells were pretreated with PKCθ pseudosubstrate peptide inhibitor and stimulated with PMA (left) or by plate-bound anti-CD3 antibodies (right) for 30 min. DCFDA oxidation was measured by FACS and presented as the increase in MFI. (G) Jurkat cells were transfected with scrambled (ctr) or PKCθ siRNA (PKCθ) oligonucleotides (as described for panel E). Cells were stimulated with PMA/ionomycin. After 1 h, RNA was isolated, reverse transcribed, and amplified with CD95L- and actin-specific primers.

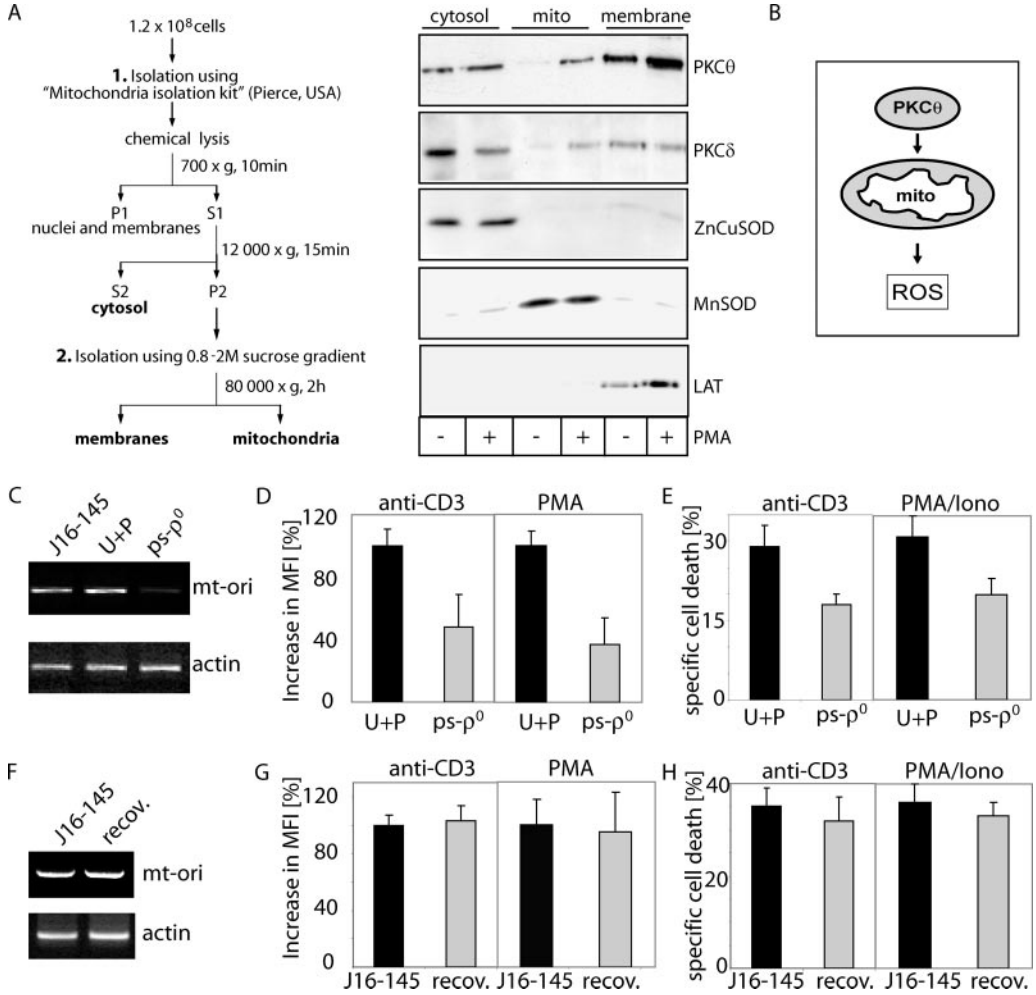

FIG. 4. PKCθ is translocated toward mitochondria upon PMA treatment. (A) J16-145 cells were stimulated with PMA for 10 min. Cells were lysed and cellular fractions were separated as depicted in the diagram (S1, S2, respective supernatants; P1, P2, respective pellets). Highlighted fractions were separated by SDS-PAGE and analyzed by Western blotting for content of PKCθ, PKCδ, ZnCuSOD (cytoplasmic marker), MnSOD (mitochondrial marker), and LAT (plasma membrane marker). (B) Schematic diagram of PKCθ translocation and ROS induction. (C to H) Involvement of mtDNA-encoded proteins in activation-induced ROS generation and AICD. (C) Total cellular DNA was isolated from parental J16-145 cells, J16-145 cells cultured in the presence of uridine (50 μg/ml) and pyruvate (110 mg/ml) (U+P), and J16-145 cells cultured in the presence of uridine plus pyruvate and ethidium bromide (250 ng/ml) (ps-ρ^0). For PCR amplification of the origin of replication of mitochondrial heavy-strand DNA (mt-ori), 100 ng of DNA template was used (upper panel). Amplification of the β-actin gene fragment was used as a loading control (lower panel). (D) Cells depleted of mtDNA show an impaired activation-induced ROS. Parental J16-145 cells cultured in medium supplemented with uridine plus pyruvate (U+P) or cells depleted of mtDNA (ps-ρ^0) were stimulated via plate-bound anti-CD3 antibodies (left) or with PMA (right) for 30 min, stained with DCFDA, and analyzed by FACS. The percent increase in MFI is shown. (E) Cells depleted of mtDNA show lowered AICD. Cells (U+P or ps-ρ^0) as described for panel C were stimulated via plate-bound anti-CD3 antibodies or with PMA/ionomycin. After 24 h, cell death was measured by a drop in the FSC/SSC index and results were recalculated to specific cell death. (F) The content of mtDNA was tested for parental J16-145 cells or pseudo-[*rho*^{0}] cells, which regained mtDNA after long-term culture due to withdrawal of ethidium bromide from the culture medium (recov). Total cellular DNA (100 ng) was used and amplified as described for panel C. (G) Parental Jurkat J16-145 cells cultured in standard medium or pseudo-[*rho*^{0}] cells after recovery of mtDNA content (recov) were stimulated by plate-bound anti-CD3 antibodies (left) or with PMA (right) for 30 min, and activation-induced ROS production was measured as described for panel D. (H) Parental J16-145 or recovered (recov) cells were stimulated by plate-bound anti-CD3 antibodies (left panel) or with PMA/ionomycin (right panel). After 24 h, cell death was determined as described for panel E.

to mitochondria, Jurkat cells were stimulated with PMA. PKC translocation was assessed by subjecting cytoplasmic, mitochondrial, and plasma membrane fractions to immunoblotting with anti-PKC antibodies. Surprisingly, PKCδ and PKCθ were detected in the plasma membrane fraction even in unstimulated cells. However, as expected, PKCδ translocates to the mitochondria after stimulation. Interestingly, the amount of PKCθ also increases in the mitochondrial fraction upon PMA treatment (Fig. 4A). Thus, PKCθ and PKCδ are translocated to the mitochondria and/or associated membranes in T cells after activation (Fig. 4B). In order to analyze the role of mitochondria in activation-induced ROS generation in more detail, cells transiently depleted of mtDNA, pseudo-[*rho*^{0}] cells, were generated by short exposure (6 to 21 days) to small amounts of ethidium bromide (Fig. 4C) (12, 36). Upon stimulation with anti-CD3 or PMA, pseudo-[*rho*^{0}] cells exhibited an up to 60%

diminished oxidative signal (Fig. 4D). Since the activation-induced oxidative signal is crucial for AICD, pseudo-[*rho*^{0}] cells displayed a massive reduction of AICD upon TCR stimulation and PMA/ionomycin treatment (Fig. 4E). The depletion of mtDNA was entirely reversible after removal of ethidium bromide from cell culture for 21 to 23 days (Fig. 4F). In concordance with the recovery of mitochondrial protein expression, activation-induced ROS generation (Fig. 4G) and AICD (Fig. 4H) regained normal levels. Thus, we demonstrate here that mitochondrial function is a prerequisite for induction of AICD.

Complex I of the mitochondrial ETC is the source of activation-induced ROS formation. Since depletion of mtDNA leads to a decrease in activation-induced ROS generation, mtDNA-encoded proteins must be involved in oxidative signaling. Most enzymes of the ETC are oligomeric complexes consisting of both nuclear DNA- and mtDNA-encoded subunits. The primary sites for mitochondrial ROS production are complexes I and III of the ETC (45). Therefore, we aimed at analyzing the role of these complexes in activation-induced ROS production. Complex I was blocked by rotenone, a commonly used inhibitor. However, rotenone is also known to interfere with a couple of cellular pathways, including tubulin-dependent signaling events (8, 16, 32, 52). Thus, we also used a second, more specific inhibitor, piericidin A (13, 28). Complex II was inhibited by the application of 1,1,1-thenoyl trifluoroacetone (TTFA), complex III by antimycin A, and complex IV by sodium azide, and the F_oF_1 ATPase was blocked by oligomycin. Cells were pretreated with these inhibitors and subsequently stimulated with anti-CD3 antibodies or PMA. Thereafter, generation of ROS was determined. Only rotenone and piericidin A were able to inhibit activation-induced ROS generation, whereas TTFA, antimycin A, sodium azide, and oligomycin had no effect on or increased the oxidative signal (Fig. 5A and B). ATP levels could not account for inhibition of ROS generation, since oligomycin and antimycin A treatment resulted in a more-efficient ATP depletion than did rotenone and piericidin A (Fig. 5C). In contrast to inhibition of the NADPH oxidase (maximum 60% blockage of ROS generation [Fig. 3]), inhibition of complex I leads to a blockage of more than 95% of activation-induced ROS production (Fig. 5A and B). Therefore, complex I is not only the source of mitochondrion-derived ROS; its activity also seems to be a prerequisite for subsequent ROS production via the NADPH oxidase.

Activation-induced ROS enhances the expression and activity of mitochondrial MnSOD. It has been demonstrated that complex I releases superoxide anion ($O_2^{\cdot -}$) into the mitochondrial matrix (65). However, it is cytosolic H_2O_2 which plays a crucial role in CD95L expression (25). Because $O_2^{\cdot -}$ cannot cross membranes (53) and leave the mitochondria, it must be converted to membrane-permeable H_2O_2 by MnSOD to act as a second messenger in the induction of AICD. To analyze whether TCR stimulation and PMA treatment result in an upregulation of MnSOD transcription, Jurkat cells were stimulated with plate-bound anti-CD3 antibodies or treated with PMA/ionomycin. RNA was isolated and reverse transcribed. After 60 min, a moderate increase in the transcript level of MnSOD was detected in CD3-stimulated and PMA/ionomycin-treated cells, whereas the cytosolic ZnCuSOD level remained unchanged (Fig. 5D). In addition, induction of MnSOD on the protein level was analyzed. Cells were stimulated with anti-CD3 antibodies or PMA/ionomycin and lysed at the indicated time points. After 4 h of stimulation, an increase in the MnSOD protein level was observed (Fig. 5E). To verify these data, the activity of MnSOD was determined. PMA treatment and CD3 stimulation led to a fast increase of MnSOD activity (Fig. 5F). Thus, complex I-derived ROS are transformed to H_2O_2 and, therefore, can serve as a second messenger in the regulation of CD95L expression (25) (Fig. 6D).

Complex I-derived ROS are crucial for the induction of CD95L expression. To analyze the role of complex I-derived ROS in activation-induced CD95L expression, we inhibited all components of the ETC. Cells were stimulated by CD3 triggering (Fig. 6A) or PMA/ionomycin treatment (Fig. 6B) in the presence or absence of inhibitors. After 1 h of treatment, RNA was isolated, reverse transcribed, and amplified with CD95L-specific primers. Significant levels of CD95L transcripts were not detected in unstimulated cells, whereas CD3 triggering and PMA/ionomycin (Fig. 6A and B) stimulation resulted in a strong expression of CD95L. The complex I inhibitors rotenone and piericidin A abolished CD95L transcription almost completely, whereas blocking of the other complexes of the ETC had no effect (Fig. 6A and B). To verify these data, a quantitative PCR was performed. Stimulation of Jurkat cells with anti-CD3 antibodies displayed a strong induction of CD95L expression. Rotenone treatment resulted in a more than 80% reduction of CD95L induction, whereas antimycin A and oligomycin showed no effect (Fig. 6C). Upon 2 h of treatment, applied doses of all inhibitors were in a subtoxic range (see Fig. 8A); thus, their toxicity cannot account for the inhibition of activation-induced ROS production and CD95L expression. Therefore, ROS generated from complex I are a prerequisite for induction of CD95L expression (Fig. 6D).

siRNA-mediated downregulation of NDUFAF1 expression inhibits activation-induced ROS signaling, CD95L expression, and AICD. In addition to pharmacological manipulation of mitochondrial respiration, we sought other ways to abolish complex I function and inhibit activation-induced ROS signaling. Mammalian complex I consists of at least 46 subunits (10); 39 of them are encoded by nuclear DNA and may be a potential target for siRNA-mediated downregulation. Recently, it was shown that NDUFAF1, a human homologue of CIA30—a complex I chaperone of *Neurospora crassa*—is essential for the assembly of complex I in humans (31, 66). Reduction of the amount of NDUFAF1 by siRNA led to lowered abundance and activity of complex I (66). To knock down NDUFAF1 expression, we used two different siRNA oligonucleotides (66). Both siRNAs displayed a knockdown effect, with siRNA oligonucleotide 2 mediating a stronger inhibition of NDUFAF1 expression (Fig. 7A). Remarkably, both oligonucleotides diminished the oxidative signal induced by PMA (oligonucleotide 1, up to 39%; oligonucleotide 2, up to 68%) (Fig. 7B and C). Since the oxidative signal generated by complex I is required for CD95L expression (Fig. 6A and B), downregulation of the NDUFAF1 level must influence transcription of CD95L. Jurkat cells transfected with NDUFAF1 siRNA oligonucleotides were stimulated with PMA/ionomycin. After 1 h of treatment, RNA was isolated, reverse transcribed, and amplified with CD95L-specific primers. Cells transfected with control oligonucleotides showed normal expression of CD95L, whereas

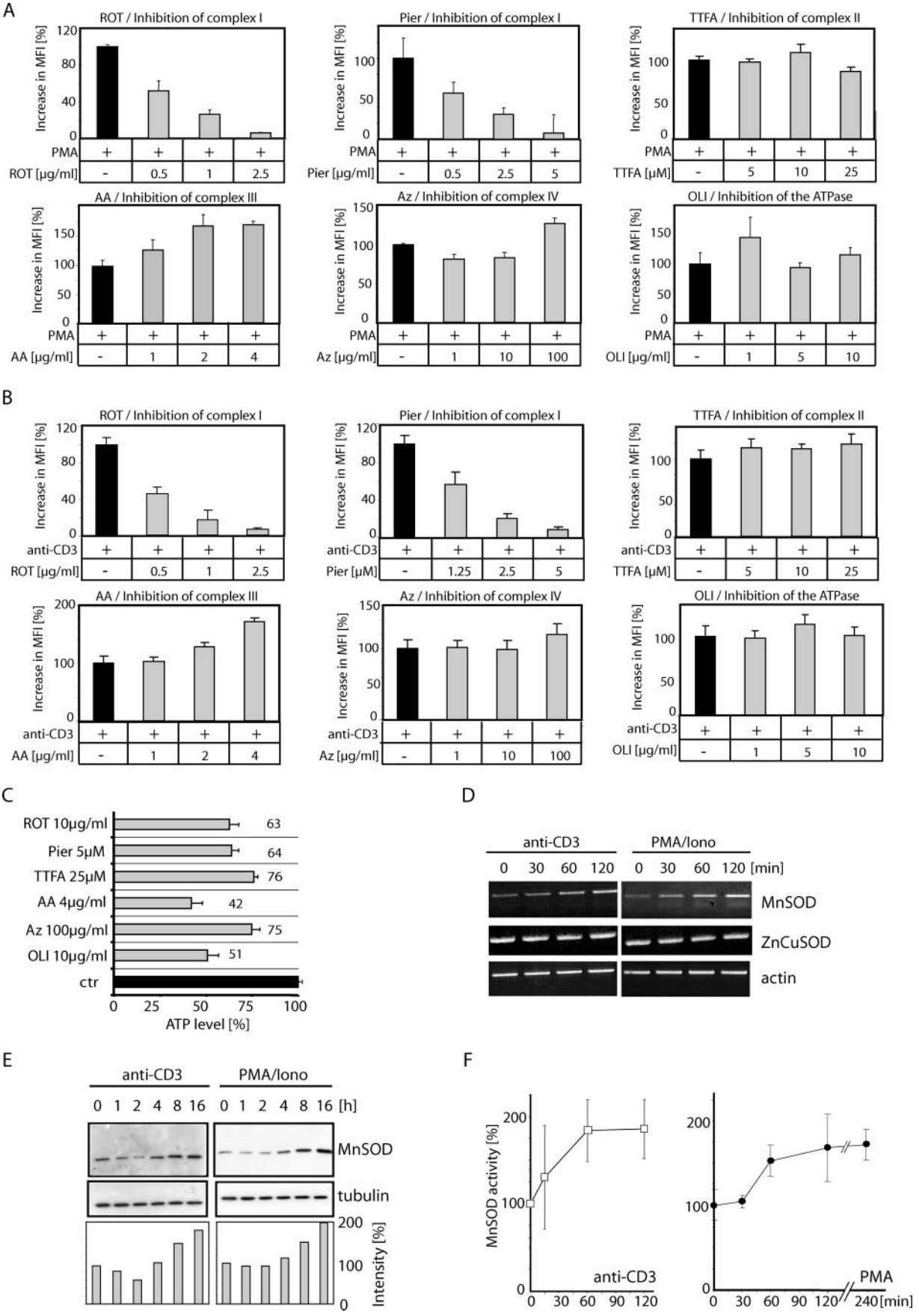
A
ROT / Inhibition of complex I
Increase in MFI [%]
PMA
ROT [μg/ml]
Pier / Inhibition of complex I
Pier [μg/ml]
TTFA / Inhibition of complex II
TTFA [μM]
AA / Inhibition of complex III
AA [μg/ml]
Az / Inhibition of complex IV
Az [μg/ml]
OLI / Inhibition of the ATPase
OLI [μg/ml]
B
anti-CD3
C
ROT 10μg/ml
Pier 5μM
TTFA 25μM
AA 4μg/ml
Az 100μg/ml
OLI 10μg/ml
ctr
ATP level [%]
D
anti-CD3
PMA/Iono
[min]
MnSOD
ZnCuSOD
actin
E
[h]
tubulin
Intensity [%]
F
MnSOD activity [%]

cells transfected with NDUFAF1 siRNA displayed strongly diminished CD95L expression (Fig. 7D). In addition, the role of complex I in AICD was analyzed in cells transfected with NDUFAF1 siRNA oligonucleotides. AICD was determined after 24 h of PMA/ionomycin treatment. In comparison to control cells, cells transfected with NDUFAF1 siRNA oligonucleotides displayed significant inhibition of cell death (Fig. 7E). Thus, we prove that complex I assembly and ROS formation are crucial for AICD induction.

Metformin inhibits complex I-derived ROS, activation-induced CD95L expression, and AICD. In search of potential tools for manipulating ROS generation at complex I and treating CD95/CD95L-dependent disorders, we applied metformin, a drug widely used in the treatment of type II diabetes (2, 3, 58). Metformin has recently received attention due to its effects on mitochondria (6, 18, 23). It has been demonstrated that metformin mildly inhibits complex I (6, 18). In addition, metformin can efficiently inhibit complex I-induced ROS production in isolated mitochondria, an effect that was linked to blockage of reversed electron flux (6). Because metformin shows no toxicity on Jurkat cells (Fig. 8A), it is an ideal tool for investigating the impact of complex I-mediated ROS production on AICD. Jurkat cells pretreated with metformin and stained with DCFDA exhibited a diminished oxidative signal after treatment with PMA (Fig. 8B). Concordantly, they also displayed an inhibition of CD95L expression upon PMA/ionomycin treatment and TCR triggering (Fig. 8C and D). A quantitative PCR revealed that cells stimulated with PMA/ionomycin and cotreated with metformin displayed a 50% reduction of CD95L expression (Fig. 8C). Even more remarkably, upon TCR triggering, metformin inhibits CD95L expression by up to 80% (Fig. 8D). AICD in Jurkat cells is mainly CD95L dependent (Fig. 8E and F). To study the effect of metformin on AICD, Jurkat cells were stimulated with either PMA/ionomycin (Fig. 8E) or plate-bound anti-CD3 antibodies (Fig. 8F). Cells pretreated with metformin showed drastically reduced AICD. Apoptosis induced via direct stimulation of the CD95 receptor was not affected by metformin (data not shown). Thus, blockage of AICD by metformin is due to inhibition of CD95L expression.

Inhibition of complex I blocks AICD in primary human T cells. To further underline the physiological relevance of complex I-derived ROS in AICD, preactivated primary human T cells (day 6 T cells) were restimulated with anti-CD3 antibodies and pretreated with or without rotenone or antimycin A. The activation-induced oxidative signal (Fig. 9A) and CD95L expression (Fig. 9B) were inhibited exclusively by rotenone. In order to prove that complex I is the source of the oxidative signal, preactivated T cells (day 6 T cells) transfected with NDUFAF1 siRNA oligonucleotides (Fig. 9C) were used to measure ROS generation upon CD3 triggering. The NDUFAF1 siRNA oligonucleotides abolished activation-induced ROS generation by up to 70% (Fig. 9D). In addition, we analyzed the effects of metformin on primary human T cells. Metformin inhibits the anti-CD3-induced oxidative signal (Fig. 9E) and induction of CD95L expression (up to 70% inhibition) (Fig. 9F). Since AICD is mainly CD95L dependent, cell death was nearly completely inhibited by metformin (Fig. 9G). In primary T cells, apoptosis induced by direct stimulation of the CD95 receptor was not affected by metformin treatment (data not shown). Thus, the nontoxic complex I inhibitor seems to be a promising tool for treatment of diseases in which deregulation of CD95L expression plays a crucial role.

DISCUSSION

The molecular source and the signaling steps necessary for ROS production are largely unknown. Here, we show for the first time that activation-induced ROS generation depends on the classical components of the TCR signaling machinery (Fig. 9H). Upon TCR stimulation LAT is phosphorylated by ZAP70 and recruits PLCγ1, which generates IP_3 and DAG. DAG, as well as its mimetic, PMA, activates several classes of enzymes, namely, PKCs, PKDs, DGKs, RasGRP, and chimearins (9). However, we show here an involvement of PKCs in activation-induced oxidative signaling. Application of BIM, a PKC-ATP binding blocker, and a specific pseudosubstrate peptide inhibited PMA- and TCR-induced ROS generation. PMA induces an oxidative signal without influencing the cytosolic Ca^{2+} level (25). Therefore, it is probable that nPKCs (calcium independent) mediate activation-induced ROS generation. Despite the fact that the nPKC isoform PKCδ is involved in ROS generation in keratinocytes and myeloid leukemia cells (39, 43), we show here that PKCθ is essential for activation-induced ROS production in T cells. Moreover, it is known that PKCθ is crucial for T-cell development and activation of the transcription factors AP-1 and NF-κB (48, 59). These transcription factors are major regulators of CD95L expression (26). In addition, AP-1 and NF-κB are ROS sensitive (17). Thus, these data are in line with the important role of PKCθ in oxidative signaling addressed in this study.

PKCs are known to activate NOX2. Recently, it was shown that human and murine T cells express NOX2. T cells from mice deficient in NOX2 displayed reduced ROS production

FIG. 5. Complex I of the mitochondrial ETC is the source of activation-induced ROS formation. (A and B) Jurkat J16-145 cells were pretreated with the indicated amounts of ETC inhibitors (ROT, rotenone; Pier, piericidin A; AA, antimycin A; TTFA, 1,1,1-thenoyl trifluoroacetone; Az, sodium azide) or an inhibitor of the F_oF_1 ATPase (OLI, oligomycin), stained with DCFDA, stimulated by PMA (A) or plate-bound anti-CD3 antibody (B) for 30 min, and analyzed by FACS. The data are presented as the percent increase in MFI. (C) Jurkat J16-145 cells were treated with high concentrations of inhibitors of the ETC or the F_oF_1 ATPase for 2 h. Thereafter, cells were lysed and ATP content was determined. (D) Mitochondrion-derived ROS induce changes in expression and activity of MnSOD. Jurkat J16-145 cells were stimulated with plate-bound anti-CD3 antibodies or PMA/ionomycin (Iono) for the indicated time periods. Isolated RNA was reverse transcribed and amplified with MnSOD-specific primers. (E) Jurkat cells were stimulated via plate-bound anti-CD3 antibodies or PMA/ionomycin (Iono) for the indicated time points. Cells were lysed and MnSOD protein levels were determined by Western blot analysis. MnSOD expression was normalized to tubulin and quantified with NIH Image (lower panel). (F) MnSOD activity in mitochondria of J16-145 cells stimulated by plate-bound anti-CD3 antibody or PMA.

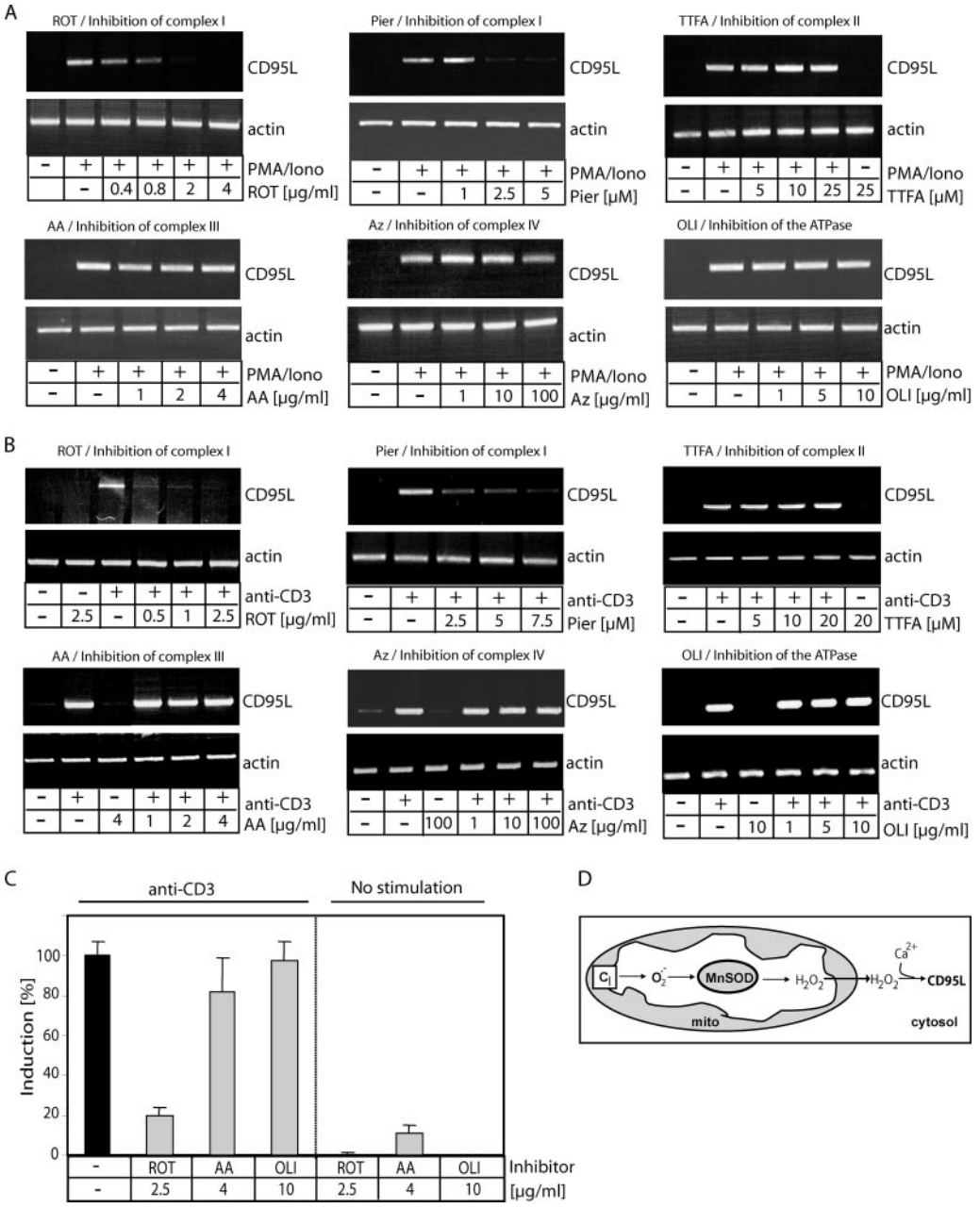

FIG. 6. ROS produced by complex I drive activation-induced CD95L expression. (A and B) J16-145 cells were pretreated with the indicated amounts of inhibitors of the ETC (ROT, rotenone; Pier, piericidin A; AA, antimycin A; TTFA, 1,1,1-thenoyl trifluoroacetone; Az, sodium azide) or the F_oF_1 ATPase (OLI, oligomycin) and stimulated with PMA/ionomycin (Iono) (A) or plate-bound anti-CD3 antibodies (B) for 1 h. RNA was isolated, reverse transcribed, and amplified with CD95L- and actin-specific primers. (C) J16-145 cells were pretreated with the indicated inhibitors and stimulated with (left) or without (right) plate-bound anti-CD3 antibodies for 1 h. RNA was isolated and reverse transcribed, and a quantitative PCR was performed. CD3-induced CD95L expression was set to 100%. All other values were calculated according to the CD3-induced CD95L expression. (D) Schematic diagram of mitochondrial ROS production. C_I, complex I.

upon TCR stimulation (30). Here, we demonstrate that NADPH oxidases participate in activation-induced ROS generation in human T cells. As with murine T cells, the oxidative signal is only partially NADPH oxidase dependent (Fig. 9H). Therefore, we focused on the identification of an additional source of ROS. Mitochondria are the most prominent intracellular source of ROS production (53). It has been reported that PKCs are translocated into/to mitochondria after PMA treatment (39, 43). Here, we show that upon activation PKCθ is translocated to the mitochondria and/or associated membrane structures. In addition, mitochondria translocate to the plasma membrane and the immunological synapse upon T-cell activation (49). To analyze the role of mitochondria in activation-induced ROS generation in more detail, we used cells transiently depleted of mtDNA, pseudo-[*rho*^{0}] cells (12, 36). These cells not only reveal a diminished activation-

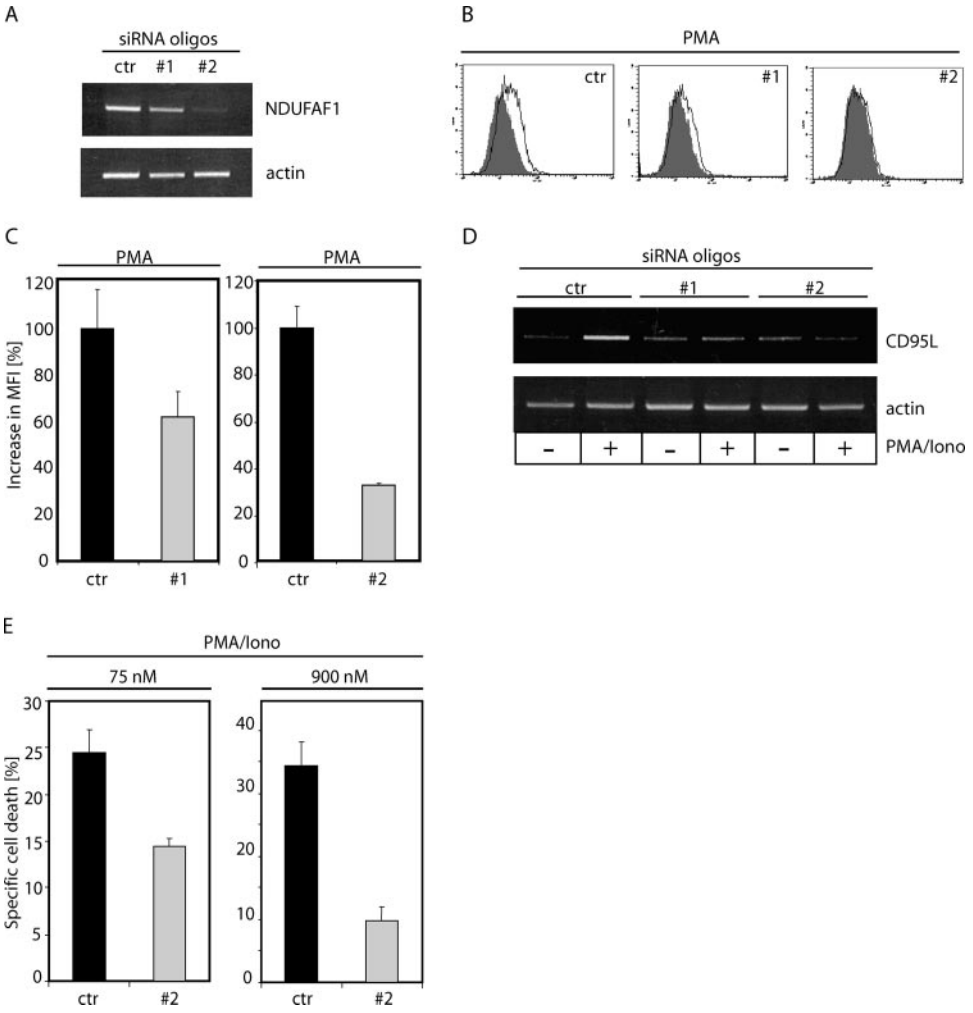

FIG. 7. Downregulation of NDUFAF1 inhibits ROS generation, CD95L expression, and AICD. (A) J16-145 cells were transfected with 75 nM concentrations of scrambled (ctr) or two different NDUFAF1-siRNA (#1 and #2) oligonucleotides. After 48 h, RNA was isolated, reverse transcribed, and amplified with NDUFAF1- and actin-specific primers. (B) At 48 h after transfection with scrambled- (ctr) or NDUFAF1-siRNA (#1 and #2) oligonucleotides, the oxidative signal upon 30 min of PMA treatment was determined by DCFDA staining (filled profile, stained cells/untreated; open profile, cells stained and stimulated with PMA). (C) Quantification of PMA-induced oxidative signals in Jurkat cells at 72 h after transfection with 75 nM concentrations of scrambled (ctr) or NDUFAF1-siRNA (#1 and #2) oligonucleotides. Cells were stained with DCFDA, treated with PMA for 30 min, and subjected to FACS analysis. Results are shown as the percent increase in MFI. (D) J16-145 cells were transfected with 75 nM concentrations of scrambled (ctr) or NDUFAF1-siRNA (#1 and #2) oligonucleotides. After 72 h of resting, cells were treated with PMA/ionomycin for 1 h. PMA/ionomycin RNA was isolated, reverse transcribed, and amplified with CD95L- and actin-specific primers. (E) J16-145 cells were transfected with 75 nM (left) or 900 nM (right) concentrations of scrambled (ctr) or NDUFAF1-siRNA (#2) oligonucleotides. After 72 h of resting, AICD was induced by 24 h of PMA/ionomycin treatment. Cell death was assessed by a drop in the FSC/SSC index. Results were recalculated to specific cell death.

induced oxidative signal but also a reduction in AICD. Therefore, we demonstrate for the first time that expression of mitochondrially encoded proteins is a prerequisite for induction of AICD.

The ETC components are oligomeric complexes consisting of both nuclear and mtDNA-encoded subunits. The primary sites for mitochondrial ROS production by the ETC are complexes I and III (45). It has been shown that rotenone, a commonly used inhibitor of complex I, interferes with $CD8^+$ T-cell function (70) and activation-induced CD95L expression (7). Nevertheless, rotenone inhibits, in addition, spindle microtubule formation and tubulin assembly, leading to cell cycle arrest, disassembly of the Golgi apparatus, disturbance of the cytoskeleton, and tubulin-dependent cell-signaling events (4, 5, 8, 16, 32, 44, 52). Therefore, it is likely that rotenone interferes with formation of the immunological synapse and movement of mitochondria. However, here we prove the role of complex I in activation-induced ROS production, CD95L expression, and AICD via downmodulation of NDUFAF1 expression (Fig. 9H). Moreover, we exclude the participation of the other complexes of the ETC in activation-induced ROS production by the use of different inhibitors. Thus, we show here that it is indeed complex I that generates ROS and is therefore responsible for the induction of CD95L expression and AICD. It is discussed whether $O_2^{\cdot -}$ (15) or H_2O_2 (25) acts as a second messenger in CD95L expression and AICD. However, complex

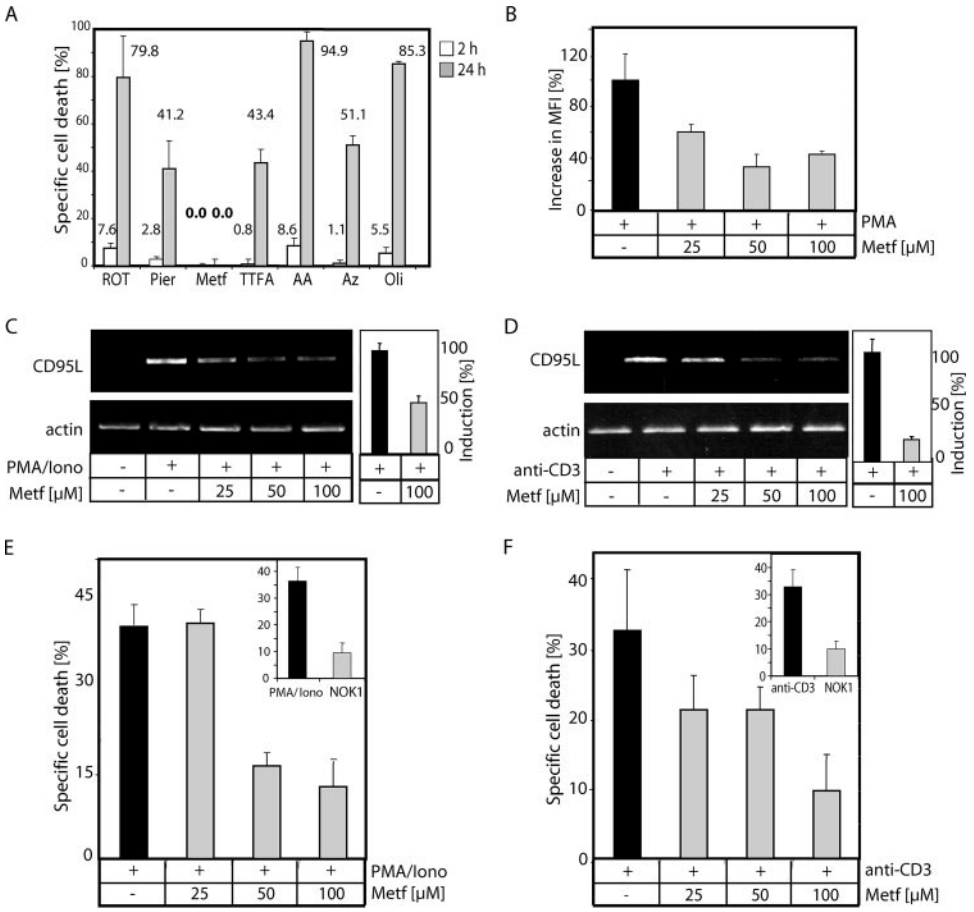

FIG. 8. Metformin, a nontoxic complex I inhibitor, blocks activation-induced oxidative signal, CD95L expression, and AICD. (A) Metformin induces no toxicity. J16-145 cells were treated for 2 h (white bars) and 24 h (gray bars) with the indicated inhibitors (ROT, rotenone [10 μg/ml]; Pier, piericidin A [7.5 μM]; Metf, metformin [100 μM]; TTFA, 1,1,1-thenoyl trifluoroacetone [25 μM]; AA, antimycin A [4 μg/ml]; Az, sodium azide [100 μg/ml]; OLI, oligomycin [10 μg/ml]). Cell death was determined by a drop in the FSC/SSC profile in comparison to living cells and recalculated to specific cell death. (B) J16-145 cells were pretreated with the indicated amounts of metformin, stained with DCFDA, and stimulated by PMA for 30 min. Oxidative signal was quantified as the increase in MFI. (C and D) J16-145 cells were pretreated with the indicated amounts of metformin and stimulated with PMA/ionomycin (Iono) (C) or plate-bound anti-CD3 antibodies (D) for 1 h. Next, RNA was isolated, reverse transcribed, and amplified with CD95L- and actin-specific primers (left). In addition, a quantitative PCR was performed (right). CD3-induced CD95L expression was set to 100%. All other values were calculated according to the CD3-induced CD95L expression. (E and F) J16-145 cells pretreated with the indicated amounts of metformin and AICD were induced by PMA/ionomycin (Iono) treatment (E) or stimulation with plate-bound anti-CD3 antibodies (F). After 24 h, cell death was assessed by the drop in the FSC/SSC index. Inserts show J16-145 cells cotreated with or without CD95L neutralizing antibody (NOK1) and stimulated by plate-bound anti-CD3 antibodies. Results were recalculated to specific cell death.

I is known to generate $O_2\cdot^-$ into the mitochondrial matrix (65). In aqueous solutions, $O_2\cdot^-$ has a half-life of less than 1 μs and is converted rapidly into H_2O_2 (53). MnSOD, an enzyme located the mitochondrial matrix, further facilitates the conversion of $O_2\cdot^-$ into H_2O_2. Here, we show that MnSOD expression and activity are enhanced upon TCR stimulation. Thus, $O_2\cdot^-$ generated by complex I is converted into H_2O_2 that can cross the mitochondrial membrane and act then as a second messenger in the cytosol. Blockage of complex I via inhibitors and siRNA-mediated downmodulation of NDUFAF1 expression leads to a nearly complete block of ROS generation. Therefore, complex I activity is crucial for subsequent NADPH oxidase-dependent ROS production (Fig. 9H). Recently, a similar connection between mitochondrial ROS generation and activation of NOX1 in 293T cells was described (38). Thus, we demonstrate that ROS produced by mitochondria, despite being known as damaging by-products of respiration, can also be released in a controlled process and serve as a second messenger.

Next, we searched for potential tools for manipulating the generation of ROS at complex I and verifying weather our findings have possible application in the treatment of CD95/CD95L-dependent diseases. Therefore, we analyzed the effect of metformin, an antidiabetic drug (2, 3, 58) and a mild inhibitor of complex I (6, 18), on AICD. Here, we demonstrate that metformin inhibits activation-induced ROS production and thereby CD95L expression and AICD. It has been shown in vitro that metformin inhibits reversed electron flux toward complex I (6). Therefore, we assume that activation-induced ROS production is coupled to reversed electron transport. Importantly, metformin is a nontoxic complex I inhibitor and therefore a potential tool for investigating diseases displaying

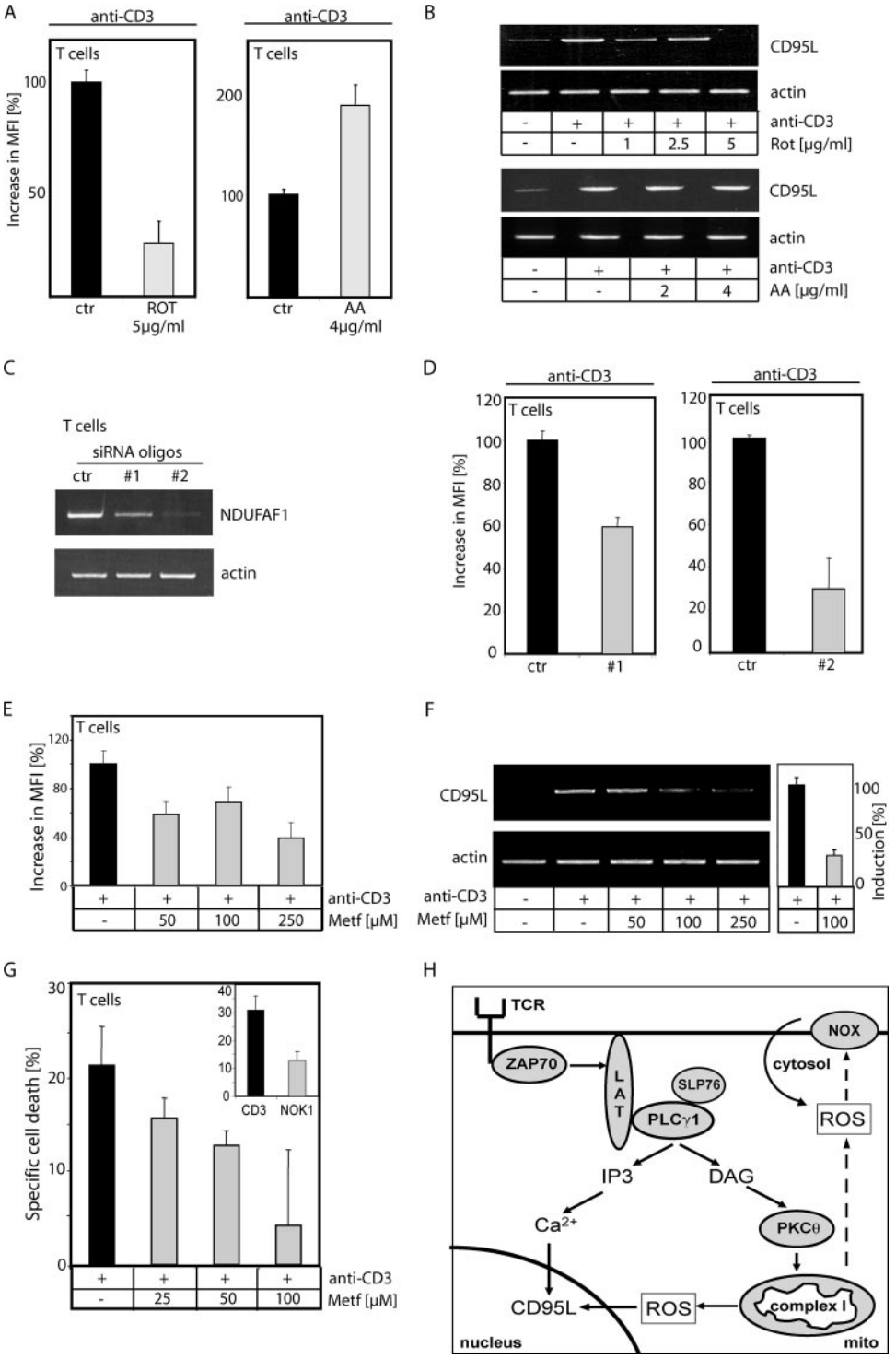

FIG. 9. Primary human T cells depend on complex I-originated activation-induced ROS for CD95L expression and AICD. (A) T cells were pretreated with the indicated amounts of inhibitors of the ETC (ROT, rotenone; AA, antimycin A) and stimulated with anti-CD3 antibodies for 30 min. Cells were stained with DCFDA, and the increase in MFI was measured by FACS. (B) T cells were pretreated with the indicated amounts of rotenone (upper panel) or antimycin A (lower panel) and stimulated with anti-CD3 antibodies for 1 h. Next, RNA was isolated, reverse transcribed, and amplified with CD95L- and actin-specific primers. (C) T cells were transfected with 900 nM scrambled (ctr) or two different NDUFAF1-siRNA (#1 and #2) oligonucleotides. After 48 h, RNA was isolated, reverse transcribed, and amplified with NDUFAF1- and actin-specific primers. (D) At 72 h after transfection with 900 nM scrambled (ctr) or NDUFAF1-siRNA (#1 and #2) oligonucleotides, primary human T cells were stimulated by plate-bound anti-CD3 antibodies for 30 min and the oxidative signal was determined as for panel A. (E to G) T cells were pretreated with the indicated amounts the nontoxic complex I inhibitor metformin and stimulated with plate-bound anti-CD3 antibodies (i) for 30 min (E), to measure the oxidative signal (quantified as in panel A); (ii) for 1 h (F), to detect changes in CD95L expression (left, semiquantitative PCR; right, quantitative PCR); or (iii) for 24 h (G), to asses AICD by a drop in the FCS/SSC index. The insert shows T cells cotreated with or without CD95L neutralizing antibody (NOK1); results were recalculated to specific cell death. (H) Schematic diagram of TCR-induced oxidative signaling.

defects in mitochondrial function combined with deregulation of CD95L expression.

AICD guards against the development of autoimmunity. Thus, the pathology of a recently reported case of fatal neonatal-onset mitochondrial respiratory chain disease with manifestation of T-cell immunodeficiency (51) could possibly be explained by our findings. Furthermore, multiple sclerosis (MS) is generally considered an anti-inflammatory disease with a substantial autoimmune contribution. On the one hand, it was shown in a genetic screening that about 20% of MS patients have mutations in mtDNA (34). It was also stated that mitochondrial complex I gene variants are associated with MS (67). On the other hand, many patients suffering from Leber's hereditary optic neuropathy disease, caused by mutations in the mitochondrially encoded subunits of complex I, display symptoms of MS (33). The MS pathology in patients with mutations in genes of complex I is not understood; therefore, our data warrant investigation of whether CD95L expression plays a role in its development. The same applies to the T-cell-specific immunodeficiency disorder associated with purine nucleoside phosphorylase deficiency, which is a result of the inhibition of mtDNA repair due to the accumulation of dGTP in mitochondria (1). Since CD95L plays an important role in T-cell development, mitochondrial damage may be responsible for impaired thymocyte differentiation in this disease. In addition, several T-cell-dependent diseases are associated with enhanced ROS levels, e.g., lupus erythematosus (47), rheumatoid arthritis (22), and AIDS (25), which influence T-cell activation, death, and homeostasis. Thus, the present findings may have further implications for the development of nontoxic inhibitors of complex I to treat diseases in which deregulation of CD95L expression or T-cell activation plays a vital role.

ACKNOWLEDGMENTS

We thank E. Fromm and M. Sohn for technical assistance and A. Tan, R. Arnold, and I. Lavrik for critical reading of the manuscript.

This project was supported by the Wilhelm Sander Stiftung, the Deutsche Forschungsgemeinschaft, and the EC.

REFERENCES

1. **Arpaia, E., P. Benveniste, A. Di Cristofano, Y. Gu, I. Dalal, S. Kelly, M. Hershfield, P. P. Pandolfi, C. M. Roifman, and A. Cohen.** 2000. Mitochondrial basis for immune deficiency. Evidence from purine nucleoside phosphorylase-deficient mice. J. Exp. Med. **191:**2197–2208.
2. **Bailey, C. J.** 1992. Biguanides and NIDDM. Diabetes Care **15:**755–772.
3. **Bailey, C. J., and R. C. Turner.** 1996. Metformin. N. Engl. J. Med. **334:**574–579.
4. **Barham, S. S., and B. R. Brinkley.** 1976. Action of rotenone and related respiratory inhibitors on mammalian cell division. 1. Cell kinetics and biochemical aspects. Cytobios **15:**85–96.
5. **Barham, S. S., and B. R. Brinkley.** 1976. Action of rotenone and related respiratory inhibitors on mammalian cell division. 2. Ultrastructural studies. Cytobios **15:**97–109.
6. **Batandier, C., B. Guigas, D. Detaille, M. Y. El-Mir, E. Fontaine, M. Rigoulet, and X. M. Leverve.** 2006. The ROS production induced by a reverse-electron flux at respiratory-chain complex 1 is hampered by metformin. J. Bioenerg. Biomembr. **38:**33–42.
7. **Bauer, M. K., M. Vogt, M. Los, J. Siegel, S. Wesselborg, and K. Schulze-Osthoff.** 1998. Role of reactive oxygen intermediates in activation-induced CD95 (APO-1/Fas) ligand expression. J. Biol. Chem. **273:**8048–8055.
8. **Brinkley, B. R., S. S. Barham, S. C. Barranco, and G. M. Fuller.** 1974. Rotenone inhibition of spindle microtubule assembly in mammalian cells. Exp. Cell Res. **85:**41–46.
9. **Brose, N., and C. Rosenmund.** 2002. Move over protein kinase C, you've got company: alternative cellular effectors of diacylglycerol and phorbol esters. J. Cell Sci. **115:**4399–4411.
10. **Carroll, J., I. M. Fearnley, J. M. Skehel, M. J. Runswick, R. J. Shannon, J. Hirst, and J. E. Walker.** 2005. The post-translational modifications of the nuclear encoded subunits of complex I from bovine heart mitochondria. Mol. Cell. Proteomics **4:**693–699.
11. **Chan, A. C., B. A. Irving, J. D. Fraser, and A. Weiss.** 1991. The zeta chain is associated with a tyrosine kinase and upon T-cell antigen receptor stimulation associates with ZAP-70, a 70-kDa tyrosine phosphoprotein. Proc. Natl. Acad. Sci. USA **88:**9166–9170.
12. **Chen, K., S. R. Thomas, A. Albano, M. P. Murphy, and J. F. Keaney, Jr.** 2004. Mitochondrial function is required for hydrogen peroxide-induced growth factor receptor transactivation and downstream signaling. J. Biol. Chem. **279:**35079–35086.
13. **Chernyak, B. V., O. Y. Pletjushkina, D. S. Izyumov, K. G. Lyamzaev, and A. V. Avetisyan.** 2005. Bioenergetics and death. Biochemistry (Moscow) **70:**240–245.
14. **Cross, A. R., and O. T. Jones.** 1986. The effect of the inhibitor diphenylene iodonium on the superoxide-generating system of neutrophils. Specific labelling of a component polypeptide of the oxidase. Biochem. J. **237:**111–116.
15. **Devadas, S., L. Zaritskaya, S. G. Rhee, L. Oberley, and M. S. Williams.** 2002. Discrete generation of superoxide and hydrogen peroxide by T cell receptor stimulation: selective regulation of mitogen-activated protein kinase activation and fas ligand expression. J Exp. Med. **195:**59–70.
16. **Diaz-Corrales, F. J., M. Asanuma, I. Miyazaki, K. Miyoshi, and N. Ogawa.** 2005. Rotenone induces aggregation of gamma-tubulin protein and subsequent disorganization of the centrosome: relevance to formation of inclusion bodies and neurodegeneration. Neuroscience **133:**117–135.
17. **Droge, W.** 2002. Free radicals in the physiological control of cell function. Physiol. Rev. **82:**47–95.
18. **El-Mir, M. Y., V. Nogueira, E. Fontaine, N. Averet, M. Rigoulet, and X. Leverve.** 2000. Dimethylbiguanide inhibits cell respiration via an indirect effect targeted on the respiratory chain complex I. J. Biol. Chem. **275:**223–228.
19. **Finco, T. S., T. Kadlecek, W. Zhang, L. E. Samelson, and A. Weiss.** 1998. LAT is required for TCR-mediated activation of PLCgamma1 and the Ras pathway. Immunity **9:**617–626.
20. **Fridovich, I.** 1970. Quantitative aspects of the production of superoxide anion radical by milk xanthine oxidase. J. Biol. Chem. **245:**4053–4057.
21. **Goldstone, S. D., A. D. Milligan, and N. H. Hunt.** 1996. Oxidative signalling and gene expression during lymphocyte activation. Biochim. Biophys. Acta **1314:**175–182.
22. **Griffiths, H. R.** 2005. ROS as signalling molecules in T cells—evidence for abnormal redox signalling in the autoimmune disease, rheumatoid arthritis. Redox Rep. **10:**273–280.
23. **Guigas, B., D. Detaille, C. Chauvin, C. Batandier, F. De Oliveira, E. Fontaine, and X. Leverve.** 2004. Metformin inhibits mitochondrial permeability transition and cell death: a pharmacological in vitro study. Biochem. J. **382:**877–884.
24. **Gulow, K., D. Bienert, and I. G. Haas.** 2002. BiP is feed-back regulated by control of protein translation efficiency. J. Cell Sci. **115:**2443–2452.
25. **Gulow, K., M. Kaminski, K. Darvas, D. Suss, M. Li-Weber, and P. H. Krammer.** 2005. HIV-1 trans-activator of transcription substitutes for oxidative signaling in activation-induced T cell death. J. Immunol. **174:**5249–5260.
26. **Gulow, K., M. Kaminski, and P. Krammer.** 2006. The role of CD95/CD95 ligand signaling in apoptosis and cancer in apoptosis and cancer therapy, part I. Wiley-VCH, Weinheim, Germany.
27. **Halliwell, B., and J. M. Gutteridge.** 1985. The importance of free radicals and catalytic metal ions in human diseases. Mol. Aspects Med. **8:**89–193.
28. **Horgan, D. J., H. Ohno, and T. P. Singer.** 1968. Studies on the respiratory chain-linked reduced nicotinamide adenine dinucleotide dehydrogenase. XV. Interactions of piericidin with the mitochondrial respiratory chain. J. Biol. Chem. **243:**5967–5976.
29. **Irvin, B. J., B. L. Williams, A. E. Nilson, H. O. Maynor, and R. T. Abraham.** 2000. Pleiotropic contributions of phospholipase C-γ1 (PLC-γ1) to T-cell antigen receptor-mediated signaling: reconstitution studies of a PLC-γ1-deficient Jurkat T-cell line. Mol. Cell. Biol. **20:**9149–9161.
30. **Jackson, S. H., S. Devadas, J. Kwon, L. A. Pinto, and M. S. Williams.** 2004. T cells express a phagocyte-type NADPH oxidase that is activated after T cell receptor stimulation. Nat. Immunol. **5:**818–827.
31. **Janssen, R., J. Smeitink, R. Smeets, and L. van Den Heuvel.** 2002. CIA30 complex I assembly factor: a candidate for human complex I deficiency? Hum. Genet. **110:**264–270.
32. **Jiang, Q., Z. Yan, and J. Feng.** 2006. Activation of group III metabotropic glutamate receptors attenuates rotenone toxicity on dopaminergic neurons through a microtubule-dependent mechanism. J. Neurosci. **26:**4318–4328.
33. **Kalman, B., and H. Alder.** 1998. Is the mitochondrial DNA involved in determining susceptibility to multiple sclerosis? Acta Neurol. Scand. **98:**232–237.
34. **Kalman, B., S. Li, D. Chatterjee, J. O'Connor, M. R. Voehl, M. D. Brown, and H. Alder.** 1999. Large scale screening of the mitochondrial DNA reveals no pathogenic mutations but a haplotype associated with multiple sclerosis in Caucasians. Acta Neurol. Scand. **99:**16–25.
35. **Keisari, Y., L. Braun, and E. Flescher.** 1983. The oxidative burst and related

phenomena in mouse macrophages elicited by different sterile inflammatory stimuli. Immunobiology **165:**78–89.
36. **King, M. P., and G. Attardi.** 1989. Human cells lacking mtDNA: repopulation with exogenous mitochondria by complementation. Science **246:**500–503.
37. **Ku, G. M., D. Yablonski, E. Manser, L. Lim, and A. Weiss.** 2001. A PAK1-PIX-PKL complex is activated by the T-cell receptor independent of Nck, Slp-76 and LAT. EMBO J. **20:**457–465.
38. **Lee, S. B., I. H. Bae, Y. S. Bae, and H. D. Um.** 2006. Link between mitochondria and NADPH oxidase 1 isozyme for the sustained production of reactive oxygen species and cell death. J. Biol. Chem. **281:**36228–36235.
39. **Li, L., P. S. Lorenzo, K. Bogi, P. M. Blumberg, and S. H. Yuspa.** 1999. Protein kinase Cδ targets mitochondria, alters mitochondrial membrane potential, and induces apoptosis in normal and neoplastic keratinocytes when overexpressed by an adenoviral vector. Mol. Cell. Biol. **19:**8547–8558.
40. **Li-Weber, M., M. Giaisi, M. K. Treiber, and P. H. Krammer.** 2002. The anti-inflammatory sesquiterpene lactone parthenolide suppresses IL-4 gene expression in peripheral blood T cells. Eur. J. Immunol. **32:**3587–3597.
41. **Li-Weber, M., O. Laur, and P. H. Krammer.** 1999. Novel Egr/NF-AT composite sites mediate activation of the CD95 (APO-1/Fas) ligand promoter in response to T cell stimulation. Eur. J. Immunol. **29:**3017–3027.
42. **Luetjens, C. M., N. T. Bui, B. Sengpiel, G. Munstermann, M. Poppe, A. J. Krohn, E. Bauerbach, J. Krieglstein, and J. H. Prehn.** 2000. Delayed mitochondrial dysfunction in excitotoxic neuron death: cytochrome c release and a secondary increase in superoxide production. J. Neurosci. **20:**5715–5723.
43. **Majumder, P. K., P. Pandey, X. Sun, K. Cheng, R. Datta, S. Saxena, S. Kharbanda, and D. Kufe.** 2000. Mitochondrial translocation of protein kinase C delta in phorbol ester-induced cytochrome c release and apoptosis. J. Biol. Chem. **275:**21793–21796.
44. **Marshall, L. E., and R. H. Himes.** 1978. Rotenone inhibition of tubulin self-assembly. Biochim. Biophys. Acta **543:**590–594.
45. **McLennan, H. R., and M. Degli Esposti.** 2000. The contribution of mitochondrial respiratory complexes to the production of reactive oxygen species. J. Bioenerg. Biomembr. **32:**153–162.
46. **Nathan, C. F., and R. K. Root.** 1977. Hydrogen peroxide release from mouse peritoneal macrophages: dependence on sequential activation and triggering. J. Exp. Med. **146:**1648–1662.
47. **Perl, A., G. Nagy, P. Gergely, F. Puskas, Y. Qian, and K. Banki.** 2004. Apoptosis and mitochondrial dysfunction in lymphocytes of patients with systemic lupus erythematosus. Methods Mol. Med. **102:**87–114.
48. **Pfeifhofer, C., K. Kofler, T. Gruber, N. G. Tabrizi, C. Lutz, K. Maly, M. Leitges, and G. Baier.** 2003. Protein kinase C theta affects Ca2+ mobilization and NFAT cell activation in primary mouse T cells. J. Exp. Med. **197:**1525–1535.
49. **Quintana, A., E. C. Schwarz, C. Schwindling, P. Lipp, L. Kaestner, and M. Hoth.** 2006. Sustained activity of calcium release-activated calcium channels requires translocation of mitochondria to the plasma membrane. J. Biol. Chem. **281:**40302–40309.
50. **Rashba-Step, J., N. J. Turro, and A. I. Cederbaum.** 1993. Increased NADPH- and NADH-dependent production of superoxide and hydroxyl radical by microsomes after chronic ethanol treatment. Arch. Biochem. Biophys. **300:**401–408.
51. **Reichenbach, J., R. Schubert, R. Horvath, J. Petersen, N. Futterer, E. Malle, A. Stumpf, B. R. Gebhardt, U. Koehl, B. Schraven, and S. Zielen.** 2006. Fatal neonatal-onset mitochondrial respiratory chain disease with T cell immunodeficiency. Pediatr. Res. **60:**321–326.
52. **Ren, Y., W. Liu, H. Jiang, Q. Jiang, and J. Feng.** 2005. Selective vulnerability of dopaminergic neurons to microtubule depolymerization. J. Biol. Chem. **280:**34105–34112.
53. **Reth, M.** 2002. Hydrogen peroxide as second messenger in lymphocyte activation. Nat. Immunol. **3:**1129–1134.
54. **Rosen, G. M., and B. A. Freeman.** 1984. Detection of superoxide generated by endothelial cells. Proc. Natl. Acad. Sci. USA **81:**7269–7273.
55. **Sanders, S. A., R. Eisenthal, and R. Harrison.** 1997. NADH oxidase activity of human xanthine oxidoreductase—generation of superoxide anion. Eur. J. Biochem. **245:**541–548.
56. **Sies, H.** 1977. Peroxisomal enzymes and oxygen metabolism in liver. Adv. Exp. Med. Biol. **78:**51–60.
57. **Stuehr, D. J., O. A. Fasehun, N. S. Kwon, S. S. Gross, J. A. Gonzalez, R. Levi, and C. F. Nathan.** 1991. Inhibition of macrophage and endothelial cell nitric oxide synthase by diphenyleneiodonium and its analogs. FASEB J. **5:**98–103.
58. **Stumvoll, M., N. Nurjhan, G. Perriello, G. Dailey, and J. E. Gerich.** 1995. Metabolic effects of metformin in non-insulin-dependent diabetes mellitus. N. Engl. J. Med. **333:**550–554.
59. **Sun, Z., C. W. Arendt, W. Ellmeier, E. M. Schaeffer, M. J. Sunshine, L. Gandhi, J. Annes, D. Petrzilka, A. Kupfer, P. L. Schwartzberg, and D. R. Littman.** 2000. PKC-theta is required for TCR-induced NF-kappaB activation in mature but not immature T lymphocytes. Nature **404:**402–407.
60. **Tew, D. G.** 1993. Inhibition of cytochrome P450 reductase by the diphenyliodonium cation. Kinetic analysis and covalent modifications. Biochemistry **32:**10209–10215.
61. **'t Hart, B. A., J. M. Simons, S. Knaan-Shanzer, N. P. Bakker, and R. P. Labadie.** 1990. Antiarthritic activity of the newly developed neutrophil oxidative burst antagonist apocynin. Free Radic. Biol. Med. **9:**127–131.
62. **Trauth, B. C., C. Klas, A. M. Peters, S. Matzku, P. Moller, W. Falk, K. M. Debatin, and P. H. Krammer.** 1989. Monoclonal antibody-mediated tumor regression by induction of apoptosis. Science **245:**301–305.
63. **Turrens, J. F., B. A. Freeman, J. G. Levitt, and J. D. Crapo.** 1982. The effect of hyperoxia on superoxide production by lung submitochondrial particles. Arch. Biochem. Biophys. **217:**401–410.
64. **Villunger, A., N. Ghaffari-Tabrizi, I. Tinhofer, N. Krumbock, B. Bauer, T. Schneider, S. Kasibhatla, R. Greil, G. Baier-Bitterlich, F. Uberall, D. R. Green, and G. Baier.** 1999. Synergistic action of protein kinase C theta and calcineurin is sufficient for Fas ligand expression and induction of a crmA-sensitive apoptosis pathway in Jurkat T cells. Eur. J. Immunol. **29:**3549–3561.
65. **Vinogradov, A. D., and V. G. Grivennikova.** 2005. Generation of superoxide-radical by the NADH:ubiquinone oxidoreductase of heart mitochondria. Biochemistry (Moscow) **70:**120–127.
66. **Vogel, R. O., R. J. Janssen, C. Ugalde, M. Grovenstein, R. J. Huijbens, H. J. Visch, L. P. van den Heuvel, P. H. Willems, M. Zeviani, J. A. Smeitink, and L. G. Nijtmans.** 2005. Human mitochondrial complex I assembly is mediated by NDUFAF1. FEBS J. **272:**5317–5326.
67. **Vyshkina, T., I. Banisor, Y. Y. Shugart, T. P. Leist, and B. Kalman.** 2005. Genetic variants of complex I in multiple sclerosis. J. Neurol. Sci. **228:**55–64.
68. **Williams, B. L., K. L. Schreiber, W. Zhang, R. L. Wange, L. E. Samelson, P. J. Leibson, and R. T. Abraham.** 1998. Genetic evidence for differential coupling of Syk family kinases to the T-cell receptor: reconstitution studies in a ZAP-70-deficient Jurkat T-cell line. Mol. Cell. Biol. **18:**1388–1399.
69. **Williamson, J. R.** 1986. Role of inositol lipid breakdown in the generation of intracellular signals. State of the art lecture. Hypertension **8**(Part II)**:**140–156.
70. **Yi, J. S., B. C. Holbrook, R. D. Michalek, N. G. Laniewski, and J. M. Grayson.** 2006. Electron transport complex I is required for CD8+ T cell function. J. Immunol. **177:**852–862.